Available online at www.sciencedirect.com

ScienceDirect

Procedia CIRP 58 (2017) 305 – 310

www.elsevier.com/locate/procedia

16th CIRP Conference on Modelling of Machining Operations

The effect of material parameters on chip formation in orthogonal cutting simulation of Ti-5553 Alloy

Melih Ozkutuk,Yusuf Kaynak*

Marmara University, Department of Mechanical Engineering, Goztepe Campus, Kadikoy-ISTANBUL-TURKEY
Marmara University, Department of Mechanical Engineering, Goztepe Campus, Kadikoy-ISTANBUL-TURKEY
* Corresponding author. Tel.: +90 216 336 5770; Fax: +90 216 337 89 87. *E-mail address:* yusuf.kaynak@marmara.edu.tr

Abstract

It is a well-known fact that Titanium alloys are commonly used materials in various industries, in particular aerospace and biomedical applications. Among titanium alloys, Ti-5553 is a new generation high temperature near beta alloy. As it has superior properties such as high tensile strength and fatigue life, it has a potential to be used in aerospace industries for structural components to replace Ti-6Al-4V. This study provides investigation on the effect of material parameters including material model parameters and frictional conditions on simulating chip formation in orthogonal cutting process of this alloy. Experimental data are used to compare forces, contact length, and to predict chip form in the cutting process of Ti-5553 alloy. This study illustrates that with calibrated frictional condition and critical damage value, it is possible to predict forces, contact length and chip morphology that can show good agreement with experimental data.

Peer-review under responsibility of the scientific committee of The 16th CIRP Conference on Modelling of Machining Operations

Keywords: Finite Element Simulation, Ti-5553 Alloy, Orthogonal Cutting

1. Introduction

Titanium alloys primarily stand out due to two properties: high specific strength and excellent corrosion resistance. This also explains their preferential use in the aerospace sector, the chemical industry and medical engineering [1]. Ti-5553 (Ti–5Al–5Mo–5V–3Cr) is a recently developed near beta Ti alloy that is gathering increasing interest in aircraft structural applications, especially in the landing gear components [2] because of their higher yield strength, excellent fatigue crack growth resistance and good hardenability [3].

However, this new refractory material presents a poor machinability compared to steel or the more known titanium alloy: Ti-6Al-4V (Ti-64) due to various reasons addressed by researchers at limited studies [4, 5] including low thermal conductivity and for this reason it is categorized as heat resistance material [6]. Some initial studies showed an important point to improve machining performance that might be useful for industry utilizing this work material [4, 7, 8]. However, to the best knowledge of authors, only two studies are available at the open literature relevant to the modeling process of this Ti-5553 alloy considering machining process. Germain et al. [9]determined the Johnson-Cook constants for this material using dynamic shear tests. Another study contributes the modeling effort of this particular alloy is presented by Sun et al. [10]. Authors presented turning processes of Ti-5553 alloys under dry and cryogenic machining conditions. Besides, they presented modeling of cutting process of this alloy by utilizing Johnson-Cook material model to predict cutting forces [10]. Although these studies are good starting point to model cutting of this alloy under various conditions, it requires further attempt to be able to predict deformation response of chip formation of this alloy under wide range of cutting conditions and to better predict response resulting from various cutting parameters.

As Ti-5553 alloys have been used to make landing gear components in aerospace industries and machining processes needed to produce these components, the development of adequate tooling and machining strategies for such alloys requires a good understanding of the thermal, mechanical and

Peer-review under responsibility of the scientific committee of The 16th CIRP Conference on Modelling of Machining Operations
doi:10.1016/j.procir.2017.03.324

microstructural aspects involved in the chip formation process [5].

Thus this study presents modeling of orthogonal cutting process of Ti-5553 alloy and exhibit simulation of cutting process at two different cutting speeds. Besides, it shows the effort made to understand the effect of frictional condition and material parameters on some outputs such as forces, contact length, and chip form in orthogonal cutting simulation of Ti-5553 alloy. Predicted forces and chip forms show good agreement with experimental data but predicted contact length shows some variation with data obtained from experimental study.

2. Experimental parameters and conditions

The work material used in this research was a Ti-5553 (Ti–5Al– 5Mo–5V–3Cr) alloy in the form of cylindrical disk of 63 mm diameter and 3 mm thickness. Cutting speeds of 60 and 120 m/min and the uncut chip thickness of 0.15 mm were used in the experimental work. Ti-5553 orthogonal machining tests were carried out on a Doosan Puma GT2100 lathe machine with 18 kW power and maximum spindle speed of 4500 rpm. It was used an uncoated carbide tool which ISO number is TCMW16T308 H13A, under dry cutting conditions to calibrate finite element model. The STNCN 2525 M16 -2 tool holder with rake angle, α= -2 degree, was used and mounted on dynamometer to measure cutting forces. Cutting forces were recorded by KISTLER 2129AA dynamometer. Experimental setup for orthogonal cutting process of Ti-5553 alloys is illustrated in Fig 1.

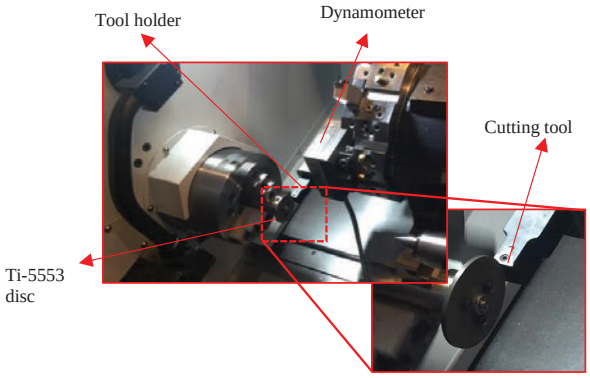

Fig. 1. Experimental setup.

3. FE Model for Orthogonal Machining

DEFORM-2D commercial software (*V11.0.2*) is used to simulate orthogonal cutting process. The created tool and its dimensional properties used in the simulation were determined considering the tool used in the experimental work. Rake angle of -2°, the cutting tool edge radius of 25 µm and a clearance angle of 7 ° are employed in the tool geometry. The cutting tool is considered to be rigid material and meshed containing 2969 elements. Also the cutting tool is modeled as uncoated and without chip breaker. The values shown in Table 1 are used for thermomechanical properties of the carbide cutting tool [11,12]. The workpiece is modeled as plastic and meshed 6122 quadrilateral elements. Mesh and boundary conditions are given in Fig. 2. Considering the cutting process, workpiece top and right side were allowed to change the heat with environment. The cutting tool's rake angle side and clearance side were allowed to change the heat with the environment. The convection coefficient was 20 W/m^{2}K which is the default value for free air convection in DEFORM 2D. Heat transfer coefficient, h_{int} at tool-chip interface was taken as 1000 kW/m^{2}K [13]. All other sides of work material and cutting tool as shown in Fig. 2 were assumed to have room temperature.

Table 1. Properties of the tool material [12].

Properties	Carbide Tool
Expansion (µm /m°C)	4.7
Density (g/cm3)	15.0
Poisson's ratio	0.20
Specific heat (J/kg/°C)	203
Conductivity (W/m°C)	46.0
Young's modulus (GPa)	800

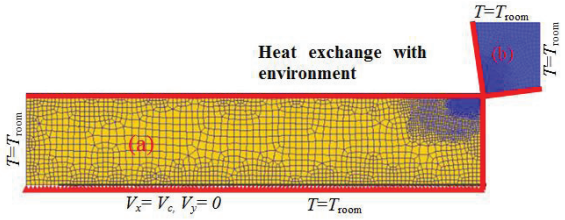

Fig.2. Mesh and boundary conditions for (a) work material, and (b) cutting tool.

The thermal conductivity of the Ti-5553 alloy material is 7.1 W/m°C [14] and the Young's modulus is defined as temperature-dependent variable and given to the Table 2.

Table 2. Young's modulus of Ti-5553 alloy [14].

T (°C)	21.11	204.44	426.66	648.88
Young's modulus (GPa)	117.2	106.8	95.1	82.7

3.1. Material modeling

To model plastic behavior of Ti-5553 alloy, Johnson-Cook constitutive equation is employed, which can be represented by the following equation [15]:

$$\bar{\sigma} = \left[A + B\left(\bar{\varepsilon}\right)^{n}\right]\left[1 + C\ln\frac{\dot{\bar{\varepsilon}}}{\dot{\bar{\varepsilon}}_0}\right]\left[1 - \left(\frac{T - T_o}{T_m - T_o}\right)^{m}\right] \quad (1)$$

In the Johnson-Cook constitution equation $\bar{\sigma}$ refers to flow stress. In this equation $\bar{\varepsilon}$, $\dot{\bar{\varepsilon}}$ and $\dot{\bar{\varepsilon}}_0$ are the strain, strain rate and reference strain rate($\dot{\bar{\varepsilon}}_0 = 1s^{-1}$)[16, 17] respectively. Workpiece temperature is expressed as T, the workpiece's melting temperature T_m(1630 °C)[10], and room temperature T_0 (20 °C). n is the hardening coefficient, m is the thermal

softening coefficient. Coefficient *A* is the yield strength, *B* is the hardening modulus, and C is the strain rate sensitivity coefficient.[15] In the Ti-5553 alloy cutting simulation, J-C was used in the model by taking the constants from the work reported by Germain et al. [9]. These constants are shown in the Table 3.

Table 3. Johnson-Cook Equation constants of Ti-5553 [9].

A(MPa)	*B*(MPa)	*n*	*m*	*C*
1175	728	0.26	1.0	0.047

3.2. Fracture criterion and friction tool/chip interface

The friction between the workpiece-tool contact is modelled using shear friction factor, m_f [18];

$$\tau = m_f . k \quad (2)$$

Here, τ is the maximum shear stress on the rake face, k is shear flow stress of the work material at the tool chip interface.

The fracture criterion for chip formation was the model proposed by Cockcroft and Latham[19];

$$\int_0^{\bar{\varepsilon}} \sigma_1 d\bar{\varepsilon} = D \quad (3)$$

ε is the effective strain; σ_1 the maximum principal stress; *D* is critical damage value that is a material constant.

Cockroft and Latham's criterion equation indicates that chip segmentation has started when the damage expression reaches critical damage value.

In order to calibrate, critical damage value and frictional conditions, various values of these were employed and cutting process of Ti-5553 is simulated to see their effect on measured outputs, particularly forces and chip form.

4. Result and discussions

4.1. Cutting force

In cutting process, one of the notable outputs is force components and predicting force components can be considerable criteria to assess the simulating capability of model utilized for cutting simulation. Figure 3 shows variation of the predicted average cutting force at two different cutting speed values as shear friction factor changes in between 0.6 to 0.8. While shear friction factor varies, critical damage value (*D*) was kept constant as 150. Predicted forces at 120 m/min are smaller than forces predicted at 60 m/min. The variation at 60 m/min cutting speed is approximately 181 N in between 0.6 to 0.8 shear friction factor, while at 120 m/min it is approximately 70 N. Variation is much higher at low cutting speed.

Predicted thrust forces at two different cutting speed shows similar trend to cutting forces, as shown in Figure 4. At lower cutting speed, the predicted thrust forces are larger than forces at higher cutting speed. The variation at 60 m/min cutting speed is larger than the variation at 120 m/min when shear friction factor is varied in between 0.6 to 0.8.

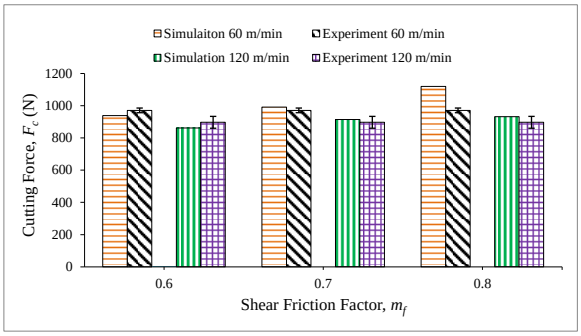

Fig.3. Experimentally measured and predicted cutting forces at two different cutting speeds.

Table 4 shows the quantitative comparison between predicted forces including cutting forces and thrust forces at 60 m/min and 120 m/min and experimentally measured force data.

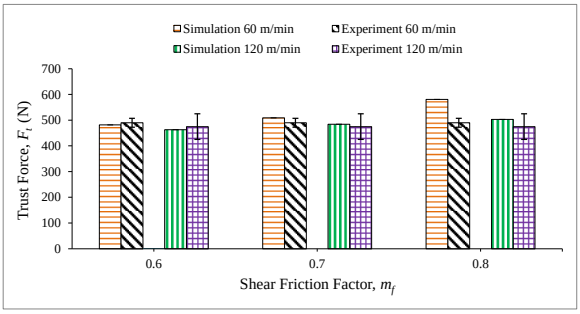

Fig.4. Experimentally measured and predicted average thrust forces at two different cutting speeds.

The largest difference in between experimental data and predicted results considering thrust force is approximately 18.6 percent when m_f=0.8 is used at 60 m/min cutting speed.

Table 4.Comparison between experimentally and predicted forces.

	F_c (N)	F_t (N)
Experimental Results (60 m/min)	971	490
Simulation m_f=0.6	939 (-3.3%)	482 (-1.6%)
Simulation m_f=0.7	991 (2.1%)	509 (3.8%)
Simulation m_f=0.8	1120 (15.3%)	581 (18.6 %)
Experimental Results (120 m/min)	897	475
Simulation m_f=0.6	862 (-3.9%)	463 (-2.5%)
Simulation m_f=0.7	914 (1.9%)	484 (1.9%)
Simulation m_f=0.8	932 (3.9%)	503 (5.9%)

Besides, the largest difference in between experimental data and predicted results considering main cutting force is approximately 15.3 percent when m_f=0.8 is used at 60 m/min cutting speed. These experimental values are the average values of forces measured and it has error bars (as shown in Figures 3 and 4) and considering this fact, it is possible to reach conclusion that model is capable of predicting experimental conditions in terms of force components.

4.2. Contact Length

Contact length is an important parameter in metal cutting process as it is related to frictional conditions in between cutting tool and chip. The images of cutting tool used in experiment and measured contact length can be seen in Figure 5(a). Predicted contact length is shown in Figure 5(b).

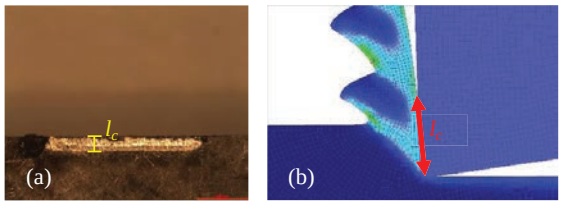

Fig.5. Demonstration of contact length a) experimental measurement b) prediction.

Figure 6 shows the effects of critical damage value (D_{CR}) on contact length. At lower critical damage values, predicted contact length at higher cutting speed is much larger than the contact length at lower cutting speed. But at the largest value of critical damage, different trend is obtained.

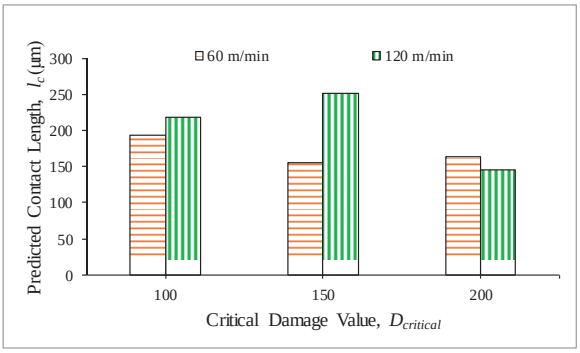

Fig.6. Predicted contact length, m_f = 0.7.

Table 5 shows the comparison between predicted contact lengths vs. experimentally measured contact length at two different cutting speeds. At lower cutting speed, the difference in between experimentally measured contact length and predicted contact length is smaller than 49 percent and the difference gets reduced as D_{CR} decreases. At higher cutting speed, the difference is much larger at in particular larger D_{CR}.

Table 5. Comparison between experimentally and predicted contact length.

	Contact Length, l_c (µm)
Experimental Results (60 m/min)	303.4
Simulation D_{CR} =100	194 (-30.1%)
Simulation D_{CR} =150	156 (-48.6%)
Simulation D_{CR} =200	163 (-46.2%)
Experimental Results (120 m/min)	329.1
Simulation D_{CR} =100	218 (-33.7%)
Simulation D_{CR} =150	252 (-23.4%)
Simulation D_{CR} =200	146 (-55.6%)

Experimentally measured contact length generally larger than predicted contact length this is mainly because of the wear occurs during experiment and enlarges contact length but in simulation, wearing of cutting tool is not taken into account

4.3. Chip Morphology

Prediction of chip morphology, namely chip thickness (t_c) and chip valley (b) resulting from three different critical damage value (D_{CR}) at two different cutting speeds are presented in this section. The predicted values of chip thickness are shown in Figure 7. It is obvious that critical damage value affects the predicted chip thickness in simulation the orthogonal cutting process of Ti-5553 alloy. At lower cutting speed, predicted chip thickness is larger as compared to higher cutting speed. Increased critical damage value leads to producing ticker chips.

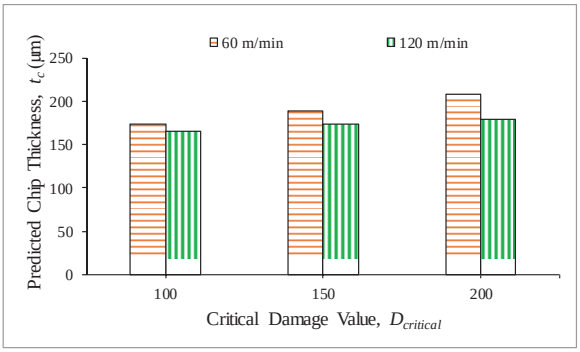

Fig.7. Predicted average chip thickness, m_f=0.7.

The chip valley results obtained from simulation at two different cutting speeds shows similar results with the predicted chip thickness. As shown in Figure 8, increased cutting speeds results in reduced chip valley at different D_{CR}. Besides, increased critical damage value leads to increased chip valley.

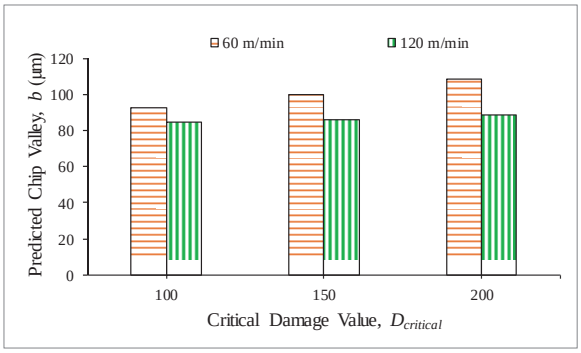

Fig.8. Predicted average chip valley, m_f = 0.7.

Experimentally generated chips at two different cutting speeds and predicted chips at these cutting speeds with various D_{CR} values are shown in Figure 9. It is obvious that segmented chips are obtained from experimental study. Simulation is capable of predicting segmented chips as well, as shown in Figure 9. The quantitative comparison of

experimentally measured chip thickness and valley and numerically predicted chip thickness and valleys resulting from two different cutting speeds are illustrated in Table 6.

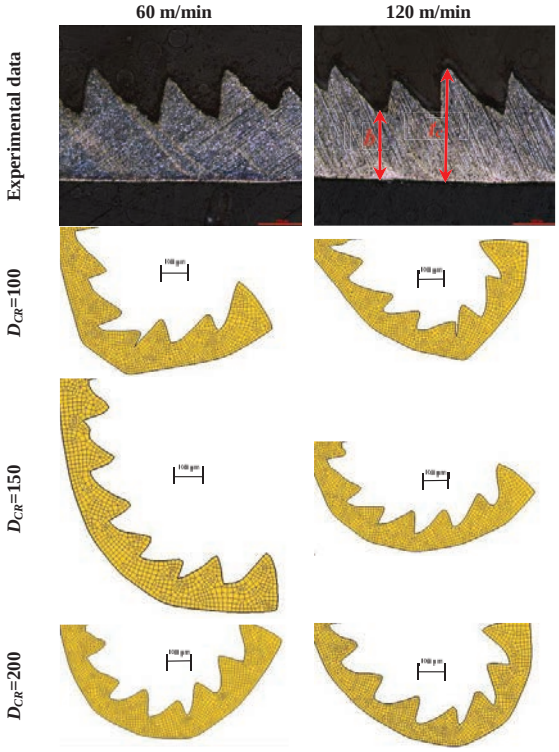

Fig.9. Comparison between experimentally obtained and predicted chip morphology, t_0 = 0.15 mm.

Simulation is capable of well predicting chip thickness and chip valley, as shown in Table 6. The largest difference in between experimentally measured chip thickness and numerically predicted one is 19.6 percent when D_{CR} = 100. The largest difference in between experimentally measured chip valley and numerically predicted one is 30.2 percent when D_{CR} = 100.

Table 6. Comparison between experimentally and predicted chip geometry.

	Chip thickness (t_c), µm	Chip valley (b), µm
Experimental Results (60 m/min)	215.6	114.1
Simulation, D_{CR} =100	173.3 (-19.6%)	92.7 (-18.7%)
Simulation, D_{CR} =150	188.4 (-12.3%)	100 (-12.6%)
Simulation , D_{CR} =200	208 (-3.5%)	108.6 (-4.7%)
Experimental Results (120 m/min)	183.8	121.8
Simulation , D_{CR} =100	165.4 (-10.0%)	85 (-30.2%)
Simulation , D_{CR} =150	173.6 (-5.5%)	86 (-29.4%)
Simulation, D_{CR} =200	179.6 (-2.3%)	89 (-26.9%)

Considering chip thickness and valley, it is possible to well predict chip thickness at D_{CR} =200 where the difference in between experimental result and simulation is lower than five percent. This show that chip thickness and valley is significantly affected from critical damage value in simulation of chip formation process of Ti-5553. Besides, cutting speed also plays an important role on generated chip morphology during simulation.

5. Conclusions

This study presents the preliminary effort to understand material parameters and frictional conditions on prediction capability of simulation of orthogonal cutting of Ti-5553 alloy. Johnson-Cook material model is utilized to simulate cutting process of Ti-5553 alloy. The predicted outputs resulting from simulation were cutting force components, contact length, and chip morphology. To improve capability of the model to predict mentioned outputs, critical damage value (D_{CR}) and frictional constant in between cutting tool and chip, m_f varied. Varying both parameters results in changes predicted output to some extent. But within selected range, simulation is well capable of capturing experimental data. In particular, within selected value of variables and using Johnson-Cook, it is possible to have very good agreement with experimental data considering forces and chip form. But it should be also noted that outputs are affected from variation of D_{CR} and m_f, but in the meantime, cutting speed also play major role to determine sensitivity of D_{CR} and m_f on predicted output. Considering overall outputs, this study shows that selecting D_{CR} = 150 and m_f =0.7 to simulate cutting process of Ti-5553 alloy can provides well capturing experimental force data. However, it is still possible to modify critical damage value to obtain much closer prediction capability for the experimental contact length and chip morphology data.

Acknowledgements

Financial support from TUBITAK (The Scientific and Technological Research Council of Turkey) under project number 214M068 is gratefully acknowledged.

References

[1] Leyens C, Peters M. Titanium and titanium alloys: Wiley Online Library; 2003.
[2] Strunk Kar SK, Ghosh A, Fulzele N, Bhattacharjee A. Quantitative microstructural characterization of a near beta Ti alloy, Ti-5553 under different processing conditions. Materials Characterization. 2013;81:37-48.
[3] Hua K, Xue X, Kou H, Fan J, Tang B, Li J. Characterization of hot deformation microstructure of a near beta titanium alloy Ti-5553. Journal of Alloys and Compounds. 2014;615:531-7.
[4] Arrazola P-J, Garay A, Iriarte L-M, Armendia M, Marya S, Le Maitre F. Machinability of titanium alloys (Ti6Al4V and Ti555. 3). Journal of materials processing technology. 2009;209(5):2223-30.
[5] Ugarte A, M'Saoubi R, Garay A, Arrazola P. Machining Behaviour of Ti-6Al-4V and Ti-5553 All0oys in Interrupted Cutting with PVD Coated Cemented carbide. Procedia CIRP. 2012;1:202-7.
[6] Wagner V, Baili M, Dessein G, Lallement D. Experimental characterization of behavior laws for titanium alloys: application to Ti5553. Key Engineering Materials: Trans Tech Publ; 2010. p. 147-55.
[7] Wagner V, Baili M, Dessein G. The relationship between the cutting speed, tool wear, and chip formation during Ti-5553 dry cutting. The International Journal of Advanced Manufacturing Technology.

2015;76(5-8):893-912.
[8] Baili M, Wagner V, Dessein G, Sallaberry J, Lallement D. An experimental investigation of hot machining with induction to improve Ti-5553 machinability. Applied mechanics and Materials: Trans Tech Publ; 2011. p. 67-76.
[9] Germain, G., A. Morel, and T. Braham-Bouchnak. Identification of material constitutive laws representative of machining conditions for two titanium alloys: Ti6Al4V and Ti555-3. Journal of Engineering Materials and Technology, 2013. 135(3): p. 031002.
[10] Sun Y, Huang B, Puleo D, Jawahir I. Enhanced Machinability of Ti-5553 Alloy from Cryogenic Machining: Comparison with MQL and Flood-cooled Machining and Modeling. Procedia CIRP. 2015;31:477-82.
[11] Kaynak Y, Manchiraju S, Jawahir, IS. Modeling and Simulation of Machining-induced Surface Integrity Characteristicsof NiTi Alloy. Procedia CIRP.2015;31: 557-562.
[12] Özel T, Zeren E. Finite element modeling the influence of edge roundness on the stress and temperature fields induced by high-speed machining. The International Journal of Advanced Manufacturing Technology. 2007;35(3-4):255-67.
[13] Filice, L., et al., On the finite element simulation of thermal phenomena in machining processes, in Advanced Methods in Material Forming. 2007, Springer. p. 263-278.
[14] Manual D. User Manual Deform-User Manual SFTC-Deform V1102,Scientific Forming Technologies Corporation Ed, Columbus, OH, USA2015.
[15] Johnson GR, Cook WH. A constitutive model and data for metals subjected to large strains, high strain rates and high temperatures. Proceedings of the 7th International Symposium on Ballistics: The Hague, The Netherlands; 1983. p. 541-7.
[16] Nemat-Nasser, S., et al., Dynamic response of conventional and hot isostatically pressed Ti–6Al–4V alloys: experiments and modeling. Mechanics of Materials, 2001. 33(8): p. 425-439.
[17] Khan, A.S., Y.S. Suh, and R. Kazmi, Quasi-static and dynamic loading responses and constitutive modeling of titanium alloys. International Journal of Plasticity, 2004. 20(12): p. 2233-2248.
[18] Ozel T. The influence of friction models on finite element simulations of machining. International Journal of Machine Tools and Manufacture 2006; 46(5): 518-530.
[19] Cockcroft M, Latham D. Ductility and the workability of metals. J Inst Metals. 1968;96(1):33-9.